

On the Origin of the Universal Radio-X-Ray Luminosity Correlation In Black Hole Candidates

Stanley L. Robertson¹ and Darryl J. Leiter²

¹*Physics Dept., Southwestern Oklahoma State University, Weatherford, OK 73096, USA (stan.robertson@swosu.edu)*

²*FSTC, Charlottesville, VA 22901, USA (dleiter@aol.com)*

2 February 2008

ABSTRACT

In previous work we found that the spectral state switch and other spectral properties of both neutron star (NS) and galactic black hole candidates (GBHC), in low mass x-ray binary systems could be explained by a magnetic propeller effect that requires an intrinsically magnetic central compact object. In later work we showed that intrinsically magnetic GBHC could be easily accommodated by general relativity in terms of magnetospheric eternally collapsing objects (MECO), with lifetimes greater than a Hubble time, and examined some of their spectral properties. In this work we show how a standard thin accretion disk and corona can interact with the central magnetic field in atoll class NS, and GBHC and active galactic nuclei (AGN) modeled as MECO, to produce jets that emit radio through infrared luminosity L_R that is correlated with mass and x-ray luminosity as $L_R \propto M^{0.75-0.92} L_x^{2/3}$ up to a mass scale invariant cutoff at the spectral state switch. Comparing the MECO-GBHC/AGN model to observations, we find that the correlation exponent, the mass scale invariant cutoff, and the radio luminosity ratios of AGN, GBHC and atoll class NS are correctly predicted, which strongly implies that GBHC and AGN have observable intrinsic magnetic moments and hence do not have event horizons.

Key words: accretion, accretion disks–black hole physics–magnetic fields–X-rays: binaries–jets and outflows–Radio continuum

1 INTRODUCTION

In earlier work (Robertson & Leiter 2002, hereafter RL02) we extended analyses of magnetic propeller effects (Campana et al. 1998, Zhang, Yu & Zhang 1998) of neutron stars (NS) in low mass x-ray binaries (LMXB) to the domain of GBHC. From the luminosities at the low/high spectral state transitions, accurate rates of spin were found for NS and accurate quiescent luminosities were calculated for *both* NS and GBHC. The NS magnetic moments were found to be consistent with $\sim 10^{8-9}$ G magnetic fields, in good agreement with those others have found (e.g. Bhattacharya 1995) from spin-down rates for similarly spinning 200 - 600 Hz millisecond pulsars. GBHC spins were found to be typically 10 - 50 Hz. Their magnetic moments of $\sim 10^{29}$ gauss cm³ are ~ 200 times larger than those of ‘atoll’ class NS (e.g. Burderi et al. 2002, DiSalvo & Burderi 2003). The implied magnetic fields of GBHC are in good agreement with fields of $\sim 10^8$ G that have been found at the base of the jets of GRS 1915+105 (Gliozzi, Bodo & Ghisellini 1999, Vadawale, Rao & Chakrabarti 2001) and in the accretion disk of Cygnus X-1 (Gnedin et al. 2003). At accretion disk inner radii corre-

sponding to the low/high spectral state switch, the magnetic fields of both ‘atoll’ class NS and GBHC are $\sim 5 \times 10^7$ G, which may account for some of their strong similarities (e.g. Yu et al. 2003, Tanaka & Shibazaki 1996, van der Klis 1994).

In later work (Leiter & Robertson 2003, Robertson & Leiter 2003, hereafter RL03) we have described how the Einstein field equations of General Relativity applied to compact plasmas with equipartition magnetic fields permit the existence of magnetic, eternally collapsing objects (MECO) that can have lifetimes in excess of a Hubble time. These highly redshifted, faintly (as distantly observed in quiescence) radiating objects can produce ‘ultrasoft’ thermal spectral peaks and the magnetic propeller effects found in RL02. Here we examine the accretion disk - magnetosphere interaction and show how the magnetosphere can drive jets. Our model should be applicable for any jet producing objects with sufficiently large magnetic moments, whether T-Tauri stars or NS, or GBHC and active galactic nuclei (AGN) modeled as MECO. In this context, the scaling of the magnetic moments of MECO with mass will be an important consideration. As shown in RL03, the MECO is dominated by a photon-photon collision generated pair plasma

which is stabilized at high redshift deep inside the photon orbit by an Eddington limit radiation pressure generated by an equipartition magnetic field intrinsic to the MECO. The surface value of the MECO intrinsic magnetic field is calculated by equating the synchrotron generated photon pressure ($\propto B^4$) to the gravitational force per unit area, which is proportional to the density. Since the density is inversely proportional to the square of the MECO mass, M , the internal magnetic field scales as $M^{-1/2}$ and the MECO magnetic moment, μ , scales as $M^{-1/2}(2GM/c^2)^3 \propto M^{5/2}$.

In the following, for NS, GBHC and AGN, we will assume the existence of a gas pressure dominated, geometrically thin accretion disk (Shakura & Sunyaev 1973). For gas pressure dominance, it has been shown (e.g., Merloni & Fabian 2002) that the hard x-ray spectral tail and reflection features of the low state spectrum can be adequately explained by reprocessing of the soft thermal disk photons in an accretion disk corona (ADC). The physical size of a corona is consistent with limits found for the source of the power-law x-ray emissions of LMXB (Church & Balucińska-Church 2003).

It has been suggested, however, (Markoff, Falcke & Fender 2001, Falcke, K rding & Markoff 2003) that the power-law x-ray emissions might originate in a jet. Flat or inverted spectrum synchrotron radio- infrared emissions are generally believed to originate in jets and low state jets have been resolved (Stirling et al. 2001) and studied over a wide range of luminosity variation (Corbel et al. 2000, 2003). As a result of these outflows, it has been pointed out (Fender, Gallo & Jonker 2003) that the low quiescent luminosities of GBHC cannot be taken as evidence of advective accretion flows (ADAF) through event horizons and as noted by Abramowicz, Kluzniak and Lasota (2002) there is presently no other observational evidence of event horizons.

Whether or not the x-rays originate in the jet, there is a strong coupling between x-ray and radio emissions that must be related to the accretion flow and jet structure. A universal low state radio / X-ray correlation ($L_R \propto L_x^{0.7}$) (Gallo, Fender & Pooley 2003) with a cutoff at the low/high state transition (Fender et al. 1999, Tannenbaum et al. 1972, Corbel et al. 2003) has been found for GBHC and NS (Migliari et al. 2003). A similar radio / x-ray correlation (Merloni, Heinz & Di Matteo 2003, Falcke, K rding & Markoff, 2003) and its suppression at the transition to the high/soft state (Maccarone, Gallo & Fender 2003) have been shown to hold for AGN as well. These radio / X-ray luminosity correlations have been examined for scale invariant jets (Heinz & Sunyaev 2003, hereafter HS03), yielding constraints on the accretion processes. In the context of HS03, Merloni, Heinz & Di Matteo (2003) (Hereafter MHD03) have examined their correlation for compatibility with various accretion flow models and found better consistency with an ADAF / jet model than with radiatively efficient disk / jet or pure jet models.

An ADAF/jet model (Meier 2001) can also account for the low/high spectral state transition as a transition from an ADAF to a standard thin disk. It relies on a rapid black hole spin to provide energy to drive the jet. The model predicts that stable high/soft states would not exist for AGN more massive than $7 \times 10^4 M_\odot$ (Meier 2001) or, with more generous allowance for hysteresis effects, $\sim 4 \times 10^6 M_\odot$ (Maccarone, Gallo & Fender 2003). The theoretical mass limit occurs be-

cause the Eddington scaled luminosity at which a thin disk (constrained to match a radiatively inefficient ADAF accretion rate) becomes radiation dominated is mass dependent. Since the high/soft state nevertheless appears to exist in AGN more massive than $6 \times 10^7 M_\odot$, the ADAF transition model cannot be regarded as established. Understanding the origin of the mass limit error of the model remains an open question (Maccarone, Gallo & Fender 2003).

Black hole models that rely entirely on the jet to produce the power-law x-ray emissions may have difficulties with constraints on the physical size of a jet. For dipping sources the size of the region of the low state power-law production has been found (Church & Balucińska-Church 2003) to be $\leq 10^9$ cm. In addition, there is the enigma of the size of the hard spectral producing region increasing while the jet dies in the high state. It is also unclear how black hole and NS behaviours could be so similar with the magnetic fields of even the weakly magnetized atoll class NS being capable of disrupting the inner accretion disk. On the other hand, we will show that our MECO model, with a radiatively efficient disk, will provide a superior fit to the radio / X-ray correlations and provide a mass scale invariant cutoff at the high/soft state transition while permitting radio-infrared and some of the x-ray luminosity to originate in a jet.

2 THE DISK - INTRINSIC MAGNETIC MOMENT INTERACTION

In the magnetic propeller model, the inner disk and magnetosphere radius, r_m , determines the spectral state. Very low to quiescent states correspond to an inner accretion disk radius outside the light cylinder. In the low/hard/radio-loud/jet-producing state of the active propeller regime, the inner disk radius lies between light cylinder and Keplerian co-rotation radii. Most, and perhaps all, of the accretion flow is ejected in the low/hard state. The high/soft state corresponds to an inner disk inside the co-rotation radius with the flow of accreting matter able to reach the central object where it produces an ultrasoft thermal spectral component. The cooling of the accretion disk corona and the former base of the jet by the soft photons also contributes to a softening of the x-ray spectrum. The whole complex of spectral state switch phenomena is related to the cessation or regeneration of magnetospherically driven outflow and presence or absence of dominant soft emissions from a central source.

The inner disk temperature is generally high enough to produce a very diamagnetic plasma at the magnetopause. Surface currents on the inner disk distort the magnetopause and they also substantially shield the trailing disk such that the region of strong disk-magnetosphere interaction is mostly confined to a ring or torus, of width δr and half height H . This shielding leaves most of the disk under the influence of its own internal shear dynamo fields, (e.g. Balbus & Hawley 1998, Balbus 2003). At the inner disk radius the magnetic field of the central MECO is much stronger than the shear dynamo field generated within the inner accretion disk. In MHD approximation, the force density on the inner ring is $F_v = (\nabla \times B) \times B/4\pi$. For simplicity, we assume coincident magnetic and spin axes of the central ob-

ject and take this axis as the z axis of cylindrical coordinates (r, ϕ, z) .

The magnetic torque per unit volume of plasma in the inner ring of the disk that is threaded by the intrinsic magnetic field of the central object, can be approximated by $\tau_v = rF_{v\phi} = r\frac{B_z}{4\pi}\frac{\partial B_\phi}{\partial z} \sim r\frac{B_z B_\phi}{4\pi H}$, where B_ϕ is the average azimuthal magnetic field component. We stress that B_ϕ , as used here, is an average toroidal magnetic field component. The toroidal component likely varies episodically between reconnection events (Goodson & Winglee 1999, Matt et al. 2002, Kato, Hayashi & Matsumoto 2004, Uzdensky 2002).

The average flow of disk angular momentum entering the inner ring is $\dot{M}rv_k$, where \dot{M} is mass accretion rate and v_k is the Keplerian speed in the disk. This angular momentum must be extracted by the magnetic torque, τ , hence:

$$\tau = \dot{M}rv_k = r\frac{B_z B_\phi}{4\pi H}(4\pi r H \delta r). \quad (1)$$

In order to proceed further, we assume that $B_\phi = \lambda B_z$, $B_z = \mu/r^3$, and use $v_k = \sqrt{GM/r}$, where λ is a constant, presumed to be of order unity, μ is the magnetic dipole moment of the central object M , its mass, and G , the Newtonian gravitational force constant. With these assumptions we obtain

$$\dot{M} = \left(\frac{\lambda \delta r}{r}\right) \frac{\mu^2}{r^5 \omega_k} \quad (2)$$

where $\omega_k = v_k/r$ and the magnetopause radius, r_m is given by

$$r_m = \left(\frac{\lambda \delta r}{r}\right)^{2/7} \left(\frac{\mu^4}{GM\dot{M}^2}\right)^{1/7} \quad (3)$$

We scale the accretion rate to that needed to produce luminosity at the Eddington limit for a central object of mass M , and define

$$\dot{m} = \frac{\dot{M}}{\dot{M}_{Edd}} \propto \frac{\dot{M}}{M} \quad (4)$$

and using $r_g = GM/c^2$ and eq. 3, we define

$$\chi = r/r_g \propto \dot{m}^{-2/7}. \quad (5)$$

In order to estimate the size of the boundary region, $(\delta r/r)$, we normalize this disk-magnetosphere model to an average atoll NS (Table 1, RL02) of mass $M = 1.4M_\odot$. The average rate of spin is ~ 450 Hz, the co-rotation radius is ~ 30 km, and the maximum luminosity for the low state is $GMM/2r \sim 2 \times 10^{36}$ erg s $^{-1}$. From this we find $\dot{M} = 6.4 \times 10^{16}$ g s $^{-1}$. Then for an average magnetic moment of $\sim 1.5 \times 10^{27}$ gauss cm 3 , we find that $(\frac{\lambda \delta r}{r})^{2/7} \sim 0.3$. Thus $\xi = \frac{\lambda \delta r}{r} \sim 0.015$; i.e., the boundary region is suitably small, though likely larger than the scale height of the trailing disk. For later convenience, we define parameters β and ξ as

$$\beta = \mu/M^3 \quad \xi = \lambda \delta r/r \quad (6)$$

Then in terms of the variables defined so far, we can express the (reprocessed) disk luminosity as

$$L_d = \frac{GMM}{2r} = \xi \frac{\sqrt{GM}\mu^2}{2r^{9/2}} = \frac{\xi \mu^2 \omega_k}{2r^3} \propto \beta^2 M^2 \dot{m}^{9/7} \quad (7)$$

At the co-rotation radius we reach the maximum luminosity, L_c , of the low/hard state, with Keplerian angular speed $\omega_k = \omega_s$, the angular speed of the magnetosphere, and $r_m = (GM/\omega_s^2)^{1/3}$. Thus

$$L_c = \xi \frac{\mu^2 \omega_s^3}{2GM} \quad (8)$$

Two additional quantities needed for the analysis of the flow into the base of a jet are the scaling parameters for the poloidal magnetic field and the inner disk density. The magnetic field at the base of the jet is simply

$$B_m = \frac{\mu}{r_m^3} \propto \frac{\beta}{\chi_m^3} \quad (9)$$

For ρ , the density in the disk, we assume a standard ‘alpha’ disk, for which $\dot{M} = \rho 4\pi r H v_r$. The radial inflow speed, v_r is proportional to $v_s H/r$, where v_s is sound speed in the disk. Using $H/r \propto v_s/v_k$, taking $v_s^2 \propto B^2/\rho$ and solving the mass flow rate equation for ρ yields:

$$\rho_m \propto \frac{\mu^2}{\dot{M} r_m^5} \propto \frac{\beta^2}{\chi_m^5} \quad (10)$$

2.1 Mass Ejection and Radio Emission

The radio luminosity of a jet is a function of the rate at which the magnetosphere can do work on the inner ring of the disk. This depends on the relative speed between the magnetosphere and the inner disk; i.e., $\dot{E} = \tau(\omega_s - \omega_k)$, or

$$\dot{E} = \xi \frac{\mu^2 \omega_s (1 - \frac{\omega_k}{\omega_s})}{r^3} \propto \mu^2 M^{-3} \dot{m}^{6/7} \omega_s (1 - \frac{\omega_k}{\omega_s}) \quad (11)$$

Disk mass, spiraling in quasi-Keplerian orbits from negligible speed at radial infinity must regain at least as much energy as was radiated away in order to escape. For this to be provided by the magnetosphere requires $\dot{E} \geq GMM/2r$, from which $\omega_k \leq 2\omega_s/3$. Thus the magnetosphere alone is incapable of completely ejecting all of the accreting matter once the inner disk reaches this limit and the radio luminosity will be commensurately reduced and ultimately cut off.¹

The radio flux, F_ν , of jet sources has a power law dependence on frequency of the form

$$F_\nu \propto \nu^{-\alpha} \quad (12)$$

The spectral energy distributions of GBHC and AGN in radio-infrared show very little, if any, evolution in the low state during outbursts; i.e., α is essentially constant ($\alpha \approx -0.5$, radio; -0.15 , IR, see e.g., Chaty et al. 2003). To determine the dependence of radio flux on μ , M and \dot{m} , we use the model and methods of HS03. Their analysis was based on a radiation transfer equation (Rybicki & Lightman 1979) which gives the radio flux from a jet viewed at right angle to the jet axis as

¹ For very rapid inner disk transit through the co-rotation radius, fast relative motion between inner disk and magnetosphere can heat the inner disk plasma and strong bursts of radiation pressure from the central object may drive large outflows while an extended jet structure is still largely intact. This process has been calculated for inner disk radii inside the marginally stable orbit (Chou & Tajima 1999) using pressures and poloidal magnetic fields of unspecified origins. A MECO is obviously capable of suppling both the field and a radiation pressure. The hysteresis of the low/high and high/low state transitions may be associated with the need for the inner disk to be completely beyond the corotation radius before a jet can be regenerated after it has subsided.

$$F_\nu \propto \int R(z)^2 j_\nu(z) [1 - \exp(-\tau_\nu(z))] / \tau_\nu(z) dz \quad (13)$$

Here z is a coordinate along the conical jet axis of symmetry, $R(z)$ is the radius of the jet, $j_\nu(z)$ is the optically thin synchrotron emissivity for a power law distribution of electrons over energy and $\tau_\nu(z)$ is the optical depth for a viewing angle perpendicular to the jet axis. Noting that $\tau_\nu(z)$ becomes huge below the shock at the base of the jet, the integral can be taken from $z \approx 0$ to $z \rightarrow \infty$. Both $j_\nu(z)$ and $\tau_\nu(z)$ depend on the magnetic field and density distributions along the jet. We assume that the magnetic field will be proportional to B_m of eq. (9). The density after passage through the jet shock will remain proportional to ρ_m of eq. (10). Thus we assume that $B(z) = \beta f(z) / \chi_m^3$ and $\rho(z) = g(z) \beta^2 / \chi_m^5$, where $f(z)$ and $g(z)$ are distribution functions along the jet.

In order to evaluate the integral for F_ν , it is helpful to scale z and $R(z)$ to match the disk radius at the base of the jet nozzle. For this purpose, we define variables scaled the same as χ ; $\zeta = z \dot{m}^{-2/7} / r_g$ and $R_\zeta(\zeta) = R(z) \dot{m}^{-2/7} / r_g$. With this scaling, R_ζ can automatically always match χ_m at the base of the jet and:

$$F_\nu \propto M^3 \dot{m}^{6/7} \int_0^\infty R_\zeta(\zeta)^2 j_\nu(\zeta) [1 - \exp(-\tau_\nu(\zeta))] / \tau_\nu(\zeta) d\zeta \quad (14)$$

The integral above has magnetic field and density dependence only via $\beta = \mu / M^3$ in Equations (9) and (10). For given inner disk radius in units of r_g , having B_m determined predominantly by the central object represents a case that was not considered in HS03. Nevertheless, using their method (and with notation adapted from their eq. (8) to the present case, $\phi_B = \beta$ and $\phi_C = \beta^2$) we obtain α from a differentiation of the logarithm of the integral with respect to $\ln(\nu)$. A second differentiation of $\ln(\alpha)$ with respect to $\ln(\dot{m})$ yields a zero because the MECO magnetic field, and thus β , is independent of \dot{m} , thus assuring that there is no low state spectral evolution as \dot{m} changes. Further, following HS03, we assume scale invariance of the jet morphology. For given χ_m , the integral is invariant with respect to \dot{m} .

The scaling of B and ρ satisfies the conditions for applicability of the method used by HS03 to obtain their eq. (10a). Then by similar method we obtain the dependence of F_ν on M and $F_\nu \propto \beta^q$, where

$$q = \frac{13 + 2p + \alpha(p + 6)}{p + 4}. \quad (15)$$

Taking the canonical value of $p = 2$, we obtain $q = (17 + 8\alpha)/6$ and for the accretion disk-intrinsic magnetic moment interaction and spectral index described by equations (1) through (14) we find

$$F_\nu \propto M^{(17+2\alpha)/6} \dot{m}^{6/7} \beta^{(17+8\alpha)/6} \nu^{-\alpha} \quad (16)$$

If $\beta \propto M^{-1/2}$, as would apply for MECO AGN/GBHC this recovers the HS03 dependence of $F_\nu \propto M^{(17/12 - \alpha/3)}$ from their eq. (10a), but for strict scale invariance of the integral, there is no further dependence on \dot{m} here. This differs from the \dot{m} dependence found by HS03 because the dominant magnetic field of the jet originates in the MECO rather than being generated in the accretion flow of the disk.

With μ in eq. (11) written in terms of β , a comparison with eq. (16) shows the radio flux to be proportional to \dot{E} . Thus we can take the integrated radio flux as luminosity, L_R , to be given by

$$L_R = C' \dot{E} = C_o M^{(2\alpha-1)/6} \beta^{(5+8\alpha)/6} \dot{E} / \omega_s \quad (17)$$

where C_o is a constant dependent on the radio bandwidth.

As noted by HS03, there will also be optically thin x-ray emission from the jet. In this case, taking $\tau_\nu \ll 1$ in eq. 14, we obtain what is essentially an integral over the jet source volume for the optically thin x-ray emission of the jet. Since $F_{\nu,x}$ depends on \dot{m} in the same way as before, both radio-infrared and the jet part of the x-ray fluxes are proportional to \dot{E} . While the base of the jet contributes to the x-ray flux, its radiating volume is likely much smaller than that of the ADC, which produces most of the x-ray flux. The cutoff of this part of the x-ray flux and the onset of soft thermal emissions as the inner disk radius pushes inside corotation and the accretion flow reaches the central object marks the spectral state transition. The ADC actually grows in the high state (while producing a declining fraction of the x-ray luminosity) as it is cooled by photons from the central object.

Finally, we note that the degree of collimation of a jet actually appears to depend on the scale height and pressure of the corona (Kato, Minishige & Shibata 2004), but F_ν can still be calculated for a largely uncollimated outflow; for example, a large angle flow spreading out from the inner rings of the disk. In this case, we would obtain an integral similar to eq. 14. with $R_\zeta^2 d\zeta$ replaced by a column length parallel to the line of sight looking into the plasma and integrated over the area of the flow, projected perpendicular to the line of sight. Though there would be differences of numerical factors depending on viewing angle, scale invariance for given $r_m/r_g = \chi_m$ would still require all coordinates to be scaled in terms of r_g and $\dot{m}^{2/7}$ in the same way as in eq. 14 and we would still obtain $F_\nu \propto \dot{E}$. Thus the scaling results we have obtained for magnetospherically driven outflows are very robust, even though there may be considerable uncertainty about the geometric details of the flow.

2.2 Radio - X-ray Correlation

Since $\dot{E} \propto r^{-3}$ and $L_d \propto r^{-9/2}$, it is apparent that we should expect radio luminosity, $L_R \propto L_d^{2/3}$. In particular we find

$$L_R = C(M, \beta, \omega_s) 2L_c^{1/3} L_d^{2/3} (1 - \omega_k / \omega_s) \quad (18)$$

where

$$C(M, \beta, \omega_s) = C_o M^{\frac{(2\alpha-1)}{6}} \beta^{\frac{(5+8\alpha)}{6}} / \omega_s \quad (19)$$

Strictly speaking, L_d should be the bolometric luminosity of the disk, however, the x-ray luminosity over a large energy band is a very substantial fraction of the disk luminosity. To compare with the correlation exponent of 2/3 obtained here, recent studies, including noisy data for both GBHC and AGN have yielded 0.71 ± 0.01 (Gallo, Fender & Pooley 2003), 0.72 (Markoff et al. 2003, Falcke, K rding & Markoff 2003), 0.60 ± 0.11 (MHD03) and 0.64 ± 0.09 (Maccarone, Gallo & Fender 2003). For α in the range 0, -0.5, $\beta \propto M^{-1/2}$, $\omega_s \propto M^{-1}$ and $L_c \propto M$, the MECO model yields $C(M) \propto M^{(9-4\alpha)/12}$ and

$$\log L_R = (2/3) \log L_x + (0.75 - 0.92) \log M + \text{const.} \quad (20)$$

which is a better fit to the "fundamental plane" of MHD03 than any of the ADAF, disk/corona or disk/jet models they considered (see their Figure 5 for a χ^2 density plot). In terms

of Eddington scaled luminosities $L_{R,Edd} = L_R/L_{Edd}$ and $L_{d,Edd} = L_d/L_{Edd}$ eq. (18) can be written as

$$L_{R,Edd} = C(M, \beta, \omega_s) 2L_{c,Edd}^{1/3} L_{x,Edd}^{2/3} (1 - \omega_k/\omega_s) \quad (21)$$

Another outstanding physical property of the MECO model for GBHC and AGN is that the Eddington scaled x-ray luminosity, L_x/L_{Edd} , which is $\propto L_c/M$ at the spectral state switch, is mass scale invariant. With μ scaling as $M^{2.5}$ and ω_s as M^{-1} , eq. (8) shows that L_c/M is constant. $L_c/L_{Edd} \approx 0.02$ has been found for GBHC and AGN (Ghisellini & Celotti 2001, Maccarone, Gallo & Fender 2003), and remarkably, a similar value is found for atoll class NS (Tanaka & Shibazaki 1996, RL02). With this common ratio, the Eddington scaled radio luminosities of MECO objects will correlate with x-ray emissions at the low/high spectral state switch in proportion to $C(M, \beta, \omega_s)$. For α in the range 0, -0.5, $C(M, \beta, \omega_s) \propto M^{0.42-0.58}$ for MECO AGN/GBHC, in good agreement with the MHD03 correlation.

Even though they are not MECO the behavior of NS x-ray binaries can also be described by our model since they contain a central object with an intrinsic magnetic moment. According to eq. 18, the ratio of peak radio luminosity to L_c is also just proportional to $C(M, \beta, \omega_s) \sim \mu^b/(M^{3b-a}\omega_s)$, where $a = (2\alpha - 1)/6$ and $b = (5 + 8\alpha)/6$. Using average values of μ, M and ω_s for the limited sample from Table 1 of RL02, and with α in the range 0, -0.5, we predict that GBHC should have peak radio / x-ray luminosity ratios that are 10 - 13 times larger than for atoll NS. Fender and Kuulkers (2001) compared the ratio of radio to x-ray luminosities at the radio peak for GBHC and NS. Omitting two GBHC and one NS that are abnormally radio loud the comparison between GBHC and atoll class NS ratio averages is $\sim 31/2.4 = 13$, from data in their Table 1.

Both L_c and peak radio emissions for Z class NS are larger because their magnetic moments are about 10X larger than those of atolls, but L_c increases by less than 10^2 , because on average they likely spin more slowly than atolls. These Z sources and abnormally loud radio sources, such as Cygnus X-3 can be explained with the magnetic model. It has been suggested that Cygnus X-3 is a NS (Brazier et al. 1990, Mitra 1998). Based on its apparent 79 Hz spin and spin down rate, it should have a magnetic moment about 13X that of an average MECO-GBHC and spin about 2.6X faster than an average MECO-GBHC (RL02). Given an adequate accretion supply, its low state steady radio emissions (not bubble events) could be $13^2 2.6^3 \sim 3000$ times stronger than an average MECO-GBHC.

If we let $x = L_d/L_c$, then for $x < 1$, corresponding to the low state, eq. (18) takes the form:

$$L_R = C(M, \beta, \omega_s) 2L_c(x^{2/3} - x) \quad (22)$$

Neglecting $C(M, \beta, \omega_s)$, the function has a maximum value of $(0.3L_c)$ at $x = 0.3$. Scaling the function for L_c at the cutoff or $0.3L_c$ at the maximum is quite easy. An ‘eyeball’ fit to the data of Figure 1 provides a sense of the sharpness of the cutoff associated with L_c . Since ω_s is known for several NS from burst oscillations, eq. (8) has been used (RL02) to constrain their magnetic moments.

L_c , in eqs. (8) and (22), is an individual cutoff luminosity that depends on ω_s , which varies, depending upon the average accretion rate produced by a binary companion or an AGN environment. Consequently the mass scale in-

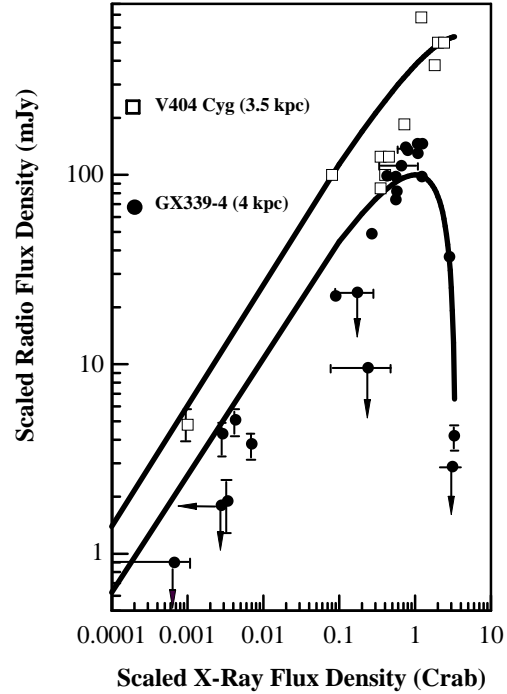


Figure 1. Radio against X-Ray flux density, scaled to a distance of 1 kpc and absorption corrected for V404 Cygni and GX 339-4. Error limits for V404 Cygni are approximately the box size, except where otherwise indicated. Lines denote fits of eq. 22 to the data. The cutoff for V404 Cygni is based on a previously identified x-ray spectral state switch (RL02). Data were kindly provided by Elena Gallo.

variant cutoff ratio L_c/L_{Edd} has a random variability, but apparently within only a narrow range. At any epoch, it is likely that most GBHC and NS are near spin equilibrium; being neither spun up nor spun down by accretion on an average over a few outburst cycles. In high states they can be spun up by accretion while in low states they are spun down by magnetospherically driven outflows. If the magnetic fields of NS weaken with age, for whatever reason, then they would be spun up commensurately by accretion disks that can then more easily penetrate to smaller radii and drive the magnetosphere to higher Keplerian angular speeds. On the other hand the highly redshifted, slow collapse of a MECO stabilizes its intrinsic equipartition magnetic field and leads us to expect very little field decay for the MECO-GBHC. Since the MECO intrinsic magnetic field is determined solely by its mass, the correct mass scaling found here for MECO-GBHC/AGN, which was based on $\omega_s \propto M^{-1}$ without additional multipliers, suggests that MECO/AGN most likely are in a state of slow spin equilibrium.

3 CONCLUSIONS

In a previous paper (RL02) we found that the spectral state switch and other spectral properties of low mass x-ray bina-

ries, including both NS and GBHC, could be explained by a magnetic propeller effect that requires an intrinsically magnetized central object. Subsequently (RL03) we applied the Einstein field equations of General Relativity to the case of a highly compact, Eddington limited, pair dominated plasma with an intrinsic equipartition magnetic field. We found that the Einstein equations permit the existence of intrinsically magnetic, highly red shifted, extremely long lived, collapsing, radiating MECO objects that can produce the required propeller effects. In addition to accounting for the strong spectral similarities of NS and GBHC, the magnetosphere-accretion disk interaction associated with the MECO model has provided explanations for radio / x-ray luminosity correlations, the mass scale invariant spectral state switch phenomenon with its suppression of the radio jet outflow in the high/ soft state, the "ultrasoft" thermal peak and hard spectral tail of the high state, and, finally, the quiescent luminosities described as spin-down driven radiations.

In conclusion, we have shown here how a standard, thin, gas pressure dominated accretion disk and corona can interact with the central intrinsic magnetic moments of MECO-GBHC/AGN and NS in x-ray binaries to drive low state jets. In the case of the MECO-GBHC/AGN the radio-infrared emissions of the jets have been found to correlate with the x-ray luminosity up to a mass scale invariant cut-off L_c/L_{Edd} at the spectral state switch. In this context we obtained radio-infrared luminosities for MECO that vary as $M^{0.75-0.92} L_x^{2/3}$, consistent with observations of GBHC and AGN, and correctly predicted the observed relative radio luminosities of NS, GBHC, and AGN. While much detailed work remains to be done, the successful comparison of the MECO model predictions with observations strongly suggests that GBHC and AGN may have observable intrinsic magnetic moments anchored within them and hence they do not have event horizons.

Acknowledgements

We thank the anonymous referee for many comments and suggestions that have substantially improved this paper. We thank Elena Gallo for providing data for Figure 1. Useful information has been generously provided by Mike Church, Heino Falcke and Thomas Maccarone. We are very grateful to Abhas Mitra for many helpful discussions of gravitational collapse and pertinent astrophysical observations.

REFERENCES

- Abramowicz, M., Kluzniak, W., Lasota, J-P, 2002 A&A 396, L31
 Balbus, S, Hawley, J, 1998 Rev. Mod. Phys. 70, 1
 Balbus, S., 2003 ARA&A 41, 555
 Bhattacharya D., 1995 in 'X-Ray Binaries', eds W. Lewin, J. van Paradijs, E. van den Heuvel, Cambridge Univ. Press
 Brazier, K. et al., 1990 ApJ 350, 745
 Burderi, L. et al., 2002 ApJ 574, 930
 Campana, S. et al., 1998 A&A Rev. 8, 279
 Chaty, S., Haswell, C., Malzac, J., Hynes, R., Shrader, C., Cui, W., 2003 MNRAS in press, astro-ph/0309047
 Chou & Tajima 1999 ApJ 513, 401
 Church, M., Balucińska-Church, 2003 MNRAS in press, astro-ph/0309212
 Corbel, S., Fender, R.P., Tzioumis, A.K., Nowak, M.A., McIntyre, V., Durouchoux, P., Sood, R., 2000 A&A 359, 251
 Corbel, S., Nowak, M.A., Fender, R.P., Tzioumis, A.K. Markoff, S., 2003 A&A 400, 1007
 Di Salvo, T., Burderi, L. 2003 A&A 397, 723
 Falcke, H., K rding, E., Markoff, S., 2003 A&A in press astro-ph/0305335
 Fender, R. et al., 1999 ApJ 519, L165
 Fender, R., Gallo, E., Jonker, P. 2003 MNRAS 343, L99
 Fender, R., Kuulkers E. 2001 MNRAS 332, 31
 Gallo, E., Fender, R., Pooley, G., 2003 MNRAS, 344, 60
 Ghisellini, G., Celotti, A., 2001 A&A 379, L1
 Gliozzi, M., Bodo, G., Ghisellini, G. 1999 MNRAS 303, L37
 Gnedin, Y. et al., 2003 Astrophys. Sp. Sci accepted, astro-ph/0304158
 Goodson, A., Winglee, R. 1999 ApJ 524, 159
 Heinz, S., Sunyaev, R., 2003 MNRAS 343, L59 (HS03)
 Kato, Y., Hayashi, M., Matsumoto, R. 2004 ApJ in press astro-ph/0308437
 Kato, Y., Minishige, S., Shibata, K., 2004 ApJ in press
 Leiter, D., Robertson, S., 2003 Found Phys. Lett. 16 143
 Maccarone, T., Gallo, E., Fender, R. 2003 MNRAS 345, L19
 Markoff, S., Falcke, H., Fender R. P., 2001 A&AL 372, L25
 Markoff, S., Nowak, M., Corbel, S., Fender, R., Falcke, H., 2003 New Astron. Rev. 47, 491
 Matt, S., Goodson, A., Winglee, R., B hm, K. 2002 ApJ 574, 232
 Meier, D., 2001 ApJ 548, L9
 Merloni, A., Fabian, A., 2002 MNRAS, 332, 165 (MHD03)
 Merloni, A., Heinz, S., Di Matteo, T., 2003 MNRAS, 345, 1057
 Migliari, S., Fender, R., Jonker, P., Klein-Wolt, M., Hjellming, R., van der Klis, M., 2003 MNRAS 342, L67
 Mitra, A. 1998 ApJ 499, 385
 Robertson, S., Leiter, D. 2002 ApJ, 565, 447 (RL02)
 Robertson, S., Leiter, D. 2003 ApJ, 596, L203 (RL03)
 Rybicki, G., Lightman, A. 1979, Radiative Processes in Astrophysics, John Wiley & Sons, New York
 Shakura, N., Sunyaev, R., 1973 A&A 24, 337
 Stirling A. M., et al., 2001 MNRAS 327, 1273
 Tanaka, Y., Shibazaki, N., 1996 ARA&A, 34, 607
 Tannenbaum, H. et al., 1972 ApJ 177, L5
 Uzdensky, D., 2002 ApJ 572, 432
 Vadawale, S., Rao, A., Chakrabarti, S. 2001 A&A 372, 793V
 van der Klis, M. 1994 ApJS 92, 511
 Yu, W., Klein-Wolt, M., Fender, R., van der Klis, M. 2003 ApJ, 589, L33
 Zhang, W., Yu, W., Zhang, S., 1998 ApJ 494, L71